Progress In Electromagnetics Research, PIER 104, 201–219, 2010

MULTIPLE ORDER DUAL-BAND ACTIVE RING FILTERS WITH COMPOSITE RIGHT/LEFT-HANDED CELLS

O. García-Pérez, L. E. García-Muñoz, and D. Segovia-Vargas

DTSC
University Carlos III de Madrid
Avda. de la Universidad 30, Leganés, Madrid 29811, Spain

V. González-Posadas

DIAC
University Politécnica de Madrid
Ctra. Valencia km. 7, Madrid 28031, Spain

Abstract—In this paper, a novel dual-band active filter topology is presented. The non-linear phase response of a composite right/left-handed cell is used to achieve the desired dual-band performance. Additionally, the proposed structure based on coupled ring resonators yields a very compact solution in which high-order implementations can be easily obtained by cascading multiple rings. The theoretical principles of this type of filters are analyzed in detail. Finally, three prototypes based on first-, second- and third-order structures validate the feasibility of this type of filters. Good agreement between simulations and measurements has been achieved.

1. INTRODUCTION

Composite right/left-handed (CRLH) transmission lines are artificial structures designed to exhibit some special properties that are not available when using conventional transmission lines [1]. They are one of the main developments in the field of metamaterials, which are electromagnetic transmission media with both negative electric permittivity and magnetic permeability. In addition to miniaturization, one of the most exploited properties of the CRLH lines is their characteristic non-linear phase response that allows the

Corresponding author: D. Segovia-Vargas (dani@tsc.uc3m.es).

design of many dual-band microwave antennas [2–4] and circuits [5–12]. Despite most contributions on CRLH lines are based on passive circuits, some multiband active devices have recently been proposed, including power amplifiers [9, 10], active diplexers [11] and active filters [12]. These circuits replace the conventional transmission lines with CRLH lines in well-known active topologies to obtain novel properties at different frequencies simultaneously.

Microwave designers have found active filters to be a very interesting solution in the design of many modern communication devices. Thus, different techniques have been developed, such as negative resistance elements [13], active inductors [14] and transversal or recursive topologies [15]. Furthermore, active filters offer responses with high Q-factors in a relatively compact size with respect to planar passive resonators. On the other hand, the emergence of many multiband services embedded in one single communication equipment makes the development of microwave components with several operation frequencies be a very powerful solution to cover this demand. With respect to dual-band active filters, a solution based on a first-order recursive structure with a CRLH line was proposed in [12]. The cited topology requires dual-band power combiners (e.g., branch-line couplers) at the input and output of the filter, what increases the overall size of the circuit and makes very difficult the practical implementation of multiple order filtering structures. Thus, no multiband and multiple order active filter topology has been previously proposed in the literature.

Microstrip ring resonators are planar filtering structures based on single or cascaded rings that offer a compact solution in the design of microwave and millimeter-wave filters [16–18]. The basic ring resonator consists of two feeding lines that are coupled to a ring, whose electrical length is a multiple of the wavelength at the desired resonance frequency. Additionally, some modifications may be introduced in this structure in order to obtain a dual-band response in different passive configurations [19–25]. On the other hand, active components can be added in the ring in order to compensate the losses introduced by the transmission lines [26]. However, no dual-band active ring filter topology has been previously presented in the literature.

In this paper, amplifiers and CRLH transmission lines are included in a ring scheme to obtain a novel active filter topology with dual-band response. Furthermore, multiple order filtering topologies are obtained by cascading several passive and active stages. Thus, the selectivity and bandwidth of the filter can be controlled by including new stages to the basic scheme. The paper is structured as follows. Section 2 presents the fundamentals of CRLH transmission lines. Some

basic concepts and considerations about active ring resonators and the proposed dual-band filter topology are explained in Section 3. Section 4 shows the main experimental results obtained with first-, second- and third-order implementations of this type of filters. Finally, the main conclusions are summarized in Section 5.

2. CRLH TRANSMISSION LINES

2.1. Transmission Line Theory

Conventional transmission lines, also known as right-handed (RH) transmission lines, can be modeled as an infinite cascaded combination of infinitesimal (i.e., $\Delta z \to 0$) LC unit cells, as the one shown in Fig. 1(a). In this case, the phase constant can be expressed as

$$\gamma_{RH} = j\omega\sqrt{L_R C_R} \tag{1}$$

where ω is the frequency, and L_R and C_R are the series per-unit-length inductance and shunt per-unit-length capacitor of the equivalent model of the right-handed line. On the other hand, a CRLH transmission line can be formed by combining the electrical models of a right-handed line and the complementary left-handed line, as can be seen in Fig. 1(b) [1]. In this case, the expression of the phase constant is given by

$$\gamma_{CRLH} = \pm j\sqrt{\left(\omega L_R - \frac{1}{\omega C_L}\right)\left(\omega C_R - \frac{1}{\omega L_L}\right)} \tag{2}$$

where ω is the frequency, and L_R is the per-unit-length series inductance, C_L is the times-unit-length series capacitance, C_R is the per-unit-length shunt capacitance and L_L is the times-unit-length inductance of the CRLH equivalent circuit model.

As it can be seen in (1), the phase response of a conventional (i.e., right-handed) transmission line describes a linear function with

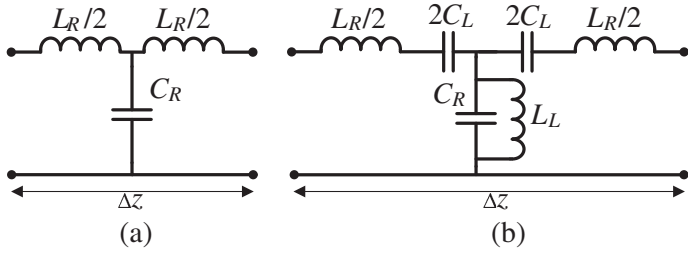

Figure 1. Unit cells for the equivalent model of (a) a right-handed transmission line and (b) a CRLH transmission line.

respect to the frequency ω. Thus, when the phase is designed to a certain value at one frequency, the phases at the rest of the frequencies are unavoidably fixed as well. This is a strong constraint for dual-band applications. However, the phase response of a CRLH transmission line is a non-linear function, as can be seen in (2). Then, there are more degrees of freedom in order to tune the phase response and exhibit two different values at two arbitrary frequencies. This property makes the use of CRLH transmission lines become very useful in the design of many dual-band circuits.

2.2. Practical Implementation

There are different possible implementations of CRLH transmission lines, depending on the final application requirements [1]. One of the most used schemes is the one combining conventional microstrip transmission lines (right-handed response) and surface mount technology lumped elements forming LC cells (left-handed response), as it can be seen in Fig. 2. By combining both responses, the global phase curve can be approximated as

$$\Phi_{CRLH} = 2\Phi_{RH} + N\frac{1}{\omega\sqrt{L'_L C'_L}} \tag{3}$$

where Φ_{RH} is the phase response of each right-handed line section, N is the number of LC cells, and L'_L and C'_L are the values of the lumped inductors and capacitors respectively (this implementation is intrinsically balanced). Therefore, it has a phase constant that is always imaginary and does not exhibit an attenuation band-gap as other implementations [1].

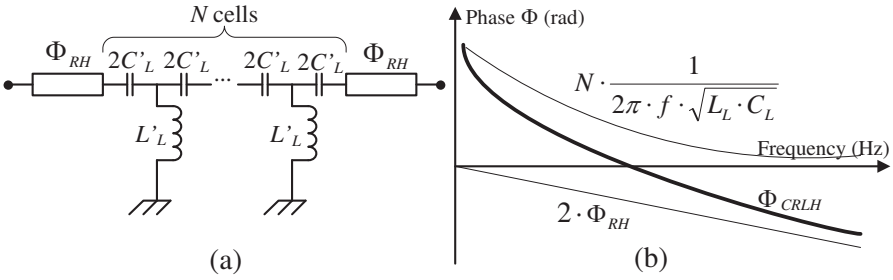

Figure 2. Physical implementation of a CRLH transmission line with (a) lumped components and conventional transmission lines and (b) the corresponding phase response.

It must be noticed that there are some implementations of CRLH lines that make use of only a few LH unit cells (e.g., [5]). Although this implementation is far from the homogenous transmission line model presented in Fig. 1(b), some authors consider this structure as a transmission line, since the overall block response presents almost all-past transmission response (as in conventional lines), but with the particularity of a non-linear phase response.

3. RING FILTERS

3.1. Conventional Ring Resonators

A typical scheme of a passive quarter-wavelength ring resonator is presented in Fig. 3(a). This topology presents a pass-band at the frequency f_0 at which the electrical length of the ring is a multiple of 2π. Furthermore, the electrical length of the coupled line combiners is chosen to be $\pi/2$ at the desired frequency to ensure a maximum coupling coefficient at this frequency. When using conventional transmission lines, the quarter-wavelength ring resonator can operate at the desired frequency f_0, and unavoidably at the odd harmonics $3f_0$, $5f_0$, etc. Thus, the circuit is not useful for dual-band applications, since it is not possible to choose the value of the second operation frequency. Some designers have also included active devices in this type of circuits to compensate the losses introduced by the transmission lines (Fig. 3(b)) [26]. In this case, the operation principles are equivalent to the ones of the passive scheme just by taking into account the phase contribution of the amplifier, as well as its noise figure, electrical

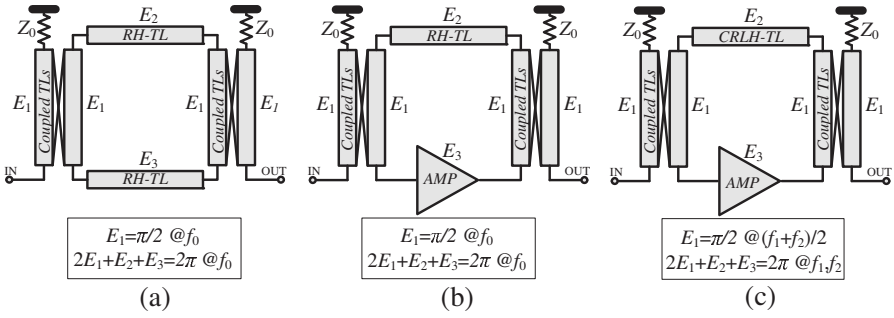

Figure 3. Ring resonator schemes: (a) Passive single-band, (b) active single-band and (c) proposed active dual-band topologies. E_i indicates the electrical length of each component, and Z_0 is the reference impedance.

stability and power consumption.

3.2. Dual-band Active Ring Resonators

In this paper the use of CRLH transmission lines in an active ring filter scheme is proposed to obtain two pass-bands at two arbitrary frequencies f_1 and f_2 (Fig. 3(c)). The phase response of this CRLH transmission line is adjusted in order to make the electrical length of the ring be a multiple of 2π at the two desired frequencies. Although the maximum coupling of the coupled lines cannot be simultaneously obtained at the two band-pass frequencies, their broadband response is, in general, enough to cover both frequencies. Finally, the sub-optimum coupling obtained at f_1 and f_2 can be compensated with the extra-gain introduced by the amplifier.

From the circuit schematic depicted in Fig. 3(c), it can be seen that there are two possible configurations depending on the branch at which the amplifier is connected, as can be seen in Fig. 4. Thus, there is a different transfer function for each one of the two topologies. Assuming perfect matching conditions between all the blocks of the circuit, the transfer function H_a for the scheme shown in Fig. 4(a), in terms of the scattering parameters, can be obtained as

$$H_a(f) = s_{21}^a(f) = \frac{A\alpha_1\alpha_2}{1 - \beta_1\beta_2\gamma A} \tag{4}$$

where f is the frequency, A is the gain function of the amplifier, α_i and β_i are the coupling and through transmission coefficients of the coupled lines, and γ is the transmission coefficient of the line. All the previous coefficients are supposed to be frequency dependent. In an equivalent mode, the transfer function H_b for the topology shown in Fig. 4(b) can be written as

$$H_b(f) = s_{21}^b(f) = \frac{\gamma\alpha_1\alpha_2}{1 - \beta_1\beta_2\gamma A} \tag{5}$$

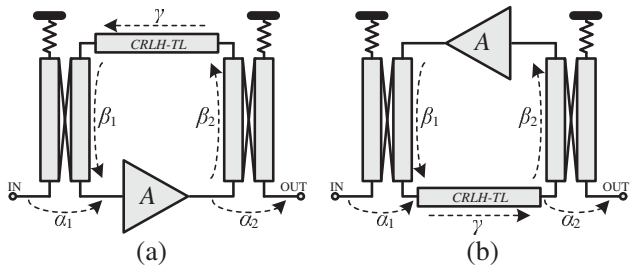

Figure 4. Two different active ring filter topologies.

Since the module of A is, in general, larger than the module of γ, the gain obtained with the first topology (i.e., H_a) will be higher than the one from the second topology (i.e., H_b) for a given set of components. Furthermore, assuming that the modules of all the transmission coefficients in the circuit remain constant with frequency, it is shown that the maximum of both transfer functions is obtained at the frequency at which the overall sum of the phases of β_1, β_2, γ and A is multiple of 2π.

3.3. Multiple Order Ring Resonators

The schemes shown in Fig. 4 correspond to first-order structures. Other higher order filtering topologies can be obtained just by combining more than one of these basic structures [26]. The general scheme on a K-order filter formed by cascading K coupled ring resonators is shown in Fig. 5. The blocks A_i and B_i are generic transmission coefficients, which may represent an amplifier or a transmission line, depending on the precise filter implementation. Assuming that the coupling coefficient of the coupled lines is much smaller than the through coefficient (i.e., $\alpha_i \ll \beta_i$), the transfer function of an K-order ring filter can be approximated by

$$H(f,K) = s_{21}(f,K) = \frac{\prod_{i=1}^{K+1} \alpha_i \prod_{j=1}^{K} A_j}{\prod_{k=1}^{K}(1-\beta_k\beta_{k+1}A_kB_k)} \tag{6}$$

In Section 4.2, two implementations of a second-order and a third-order filter based on the scheme presented in Fig. 5 will be shown.

3.4. Stability Considerations

Stability is one of the most important issues that must be addressed in any active circuit, especially when working with feedback topologies. The stability of single frequency feedback filters has been analyzed in some previous works [27], and the main results can be applied to the

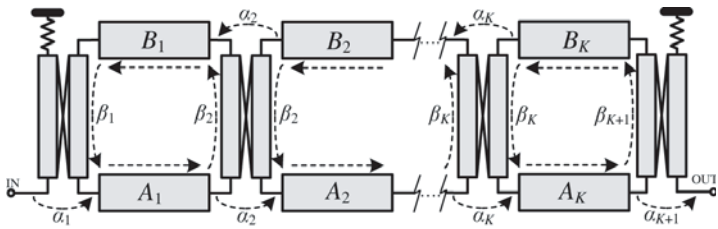

Figure 5. General scheme of a N-order ring filter.

proposed ring topology. The cited work concludes that it is necessary to limit the gain of the amplifier under a certain threshold, in order to avoid stability problems caused by an excess of gain (e.g., including resistive attenuators in the ring). In fact, there are two types of stability problems in this type of band-pass filters, both of them caused when working with non-ideal power combiners. The first case yields out-of-band instabilities that are caused by the limited bandwidth presented by some narrowband power combiners (e.g., branch line couplers [12]). In this case, there are some frequency ranges at which the combiner does not isolate the feedback line and the input, and some part of the amplified signal may be fed back to the input. On the other hand, it is possible to have stability problems inside the pass-band, even if the power combiners are operating at this frequency, because of a non perfect isolation when working with real components. Since the coupled lines used to combine the signals in this case can be considered as broadband combiners, is this second case the one to be considered in our implementations.

The transfer function H_a corresponding to the first-order ring filter presented in Fig. 4(a) can be represented at the band-pass frequency as a function of the amplifier gain $|A|$, as can be seen in Fig. 6. There is a value of $|A|$ at which the denominator of (4) becomes zero and the curve presents an asymptote. This threshold value can be calculated as

$$A_{th} = 1/(|\beta_1||\beta_2||\gamma|) \tag{7}$$

and is the value at which the gain in the ring is one. As exposed in [12], if the value of $|A|$ is higher than A_{th}, it leads to unconditionally unstable schemes. Thus, it is desirable to limit the value of $|A|$, at least,

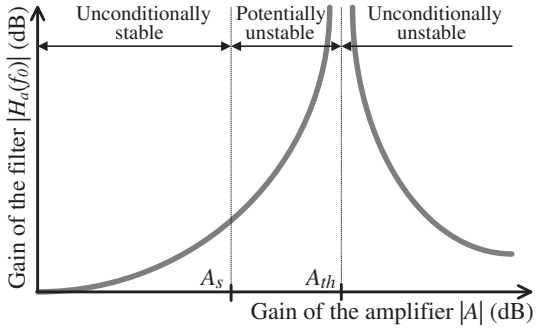

Figure 6. Transfer function (4) of a first-order active filter as a function of the gain of the amplifier and typical stability regions.

under this threshold value A_{th}, in order to avoid instabilities:

$$|A| < |A_{th}| \tag{8}$$

Lastly, even if condition (8) is fulfilled, unconditional stability is not guaranteed, especially when using values of $|A|$ closed to A_{th}. Therefore, the filter is unconditionally stable up to a certain value A_s, which is lower than A_{th}. The concrete value of A_s depends on the particular realization of the filter, and especially on some non-idealities of the components that have not been considered in the ideal scheme previously analyzed.

3.5. Noise Considerations

The noise performance of a first-order active ring filter depends on the placement of the amplifier inside the structure. Thus, there are two different expressions for each one of the topologies presented in Fig. 4. Based on the noise wave analysis developed in [28], the noise factor F_a for the scheme shown in Fig. 4(a) can be obtained as

$$F_a = 1 + \frac{1}{\alpha_1^2}(F_{amp} - 1) + \left(\frac{\beta_2 - \beta_1 A\gamma}{\alpha_1 \alpha_2 A}\right)^2 \tag{9}$$

where F_{amp} is the noise factor of the isolated amplifier. The noise factor of the topology shown in Fig. 4(b) can be obtained by the same method as

$$F_b = 1 + \left(\frac{\beta_1 A}{\alpha_1}\right)^2 (F_{amp} - 1) + \left(\frac{\beta_2 - \beta_1 A\gamma}{\alpha_1 \alpha_2 \gamma}\right)^2 \tag{10}$$

Analyzing the previous expressions (9), (10), it can be seen a strong sensitivity of the noise factor with respect to the power balance of the input and output combiners (α_i and β_i). One of the main drawbacks of the proposed ring topology is that the power balance of the coupled lines is very asymmetric ($\alpha_i \ll \beta_i$), and therefore this filtering structure will be very noisy in comparison with filters that make use of other type of combiners (e.g., 3-dB hybrids). If there were strong requirements in terms of noise, the corresponding figure could be improved by choosing a better power balance in the combiners (α_i and β_i) [28]. However, there are strong limitations when working with microstrip coupled lines since, in practice, it is very difficult to increase the coupling factor above a certain limit. Since the more critical combiner is the one connected to the input of the filter, another option is to connect a more symmetric combiner to the input (e.g., Lange coupler, Wilkinson, etc.). Thus, the noise figure of the filter can be reduced without critical costs in terms of compactness.

3.6. Broadband vs. Dual-band Power Combiners

The use of CRLH lines to achieve dual-band responses with a first-order recursive filter topology was firstly presented in [12]. That scheme used a feedback topology with branch-line couplers to combine the signals at the input and output of the filter and presented several potential drawbacks. Firstly, the size of the filter was large due to the dimensions of both combiners. Furthermore, multiple order schemes would require additional branch-line couplers for each signal combination increasing the complexity of the hypothetical filter. Finally, the phase contribution of the dual-band couplers made the feedback loop act as an electrically long path, so the electrical length of the loop is a multiple of a wavelength not only at the two desired band-pass frequencies, but also at other undesired intermediate frequencies. Thus, some spurious peaks appeared between both pass-bands in the filter response.

The use of broadband couplers and CRLH lines in a ring topology allows designing more compact dual-band active filters. Thus, the limitations coming when using other feedback topologies based on narrowband combiners are overcome. As a consequence, it is more feasible to combine more than one stage, forming higher order filters. Finally, the appearance of spurious peaks between both desired pass-bands may be avoided when using broadband combiners instead of dual-band combiners, as presented in Fig. 7. Dual-band combiners require replicating the same phase conditions at the two operating frequencies f_1 and f_2, and therefore the phase curve has to change abruptly between both frequencies (Fig. 7(c)). This response is

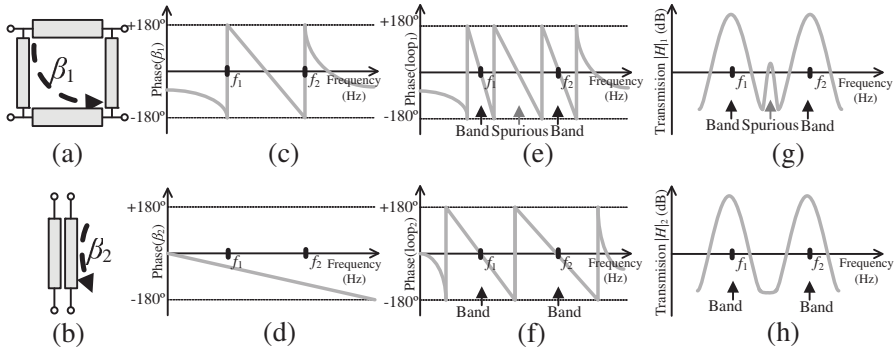

Figure 7. Comparison between feedback filters based on dual-band (top) or broadband (bottom) combiners: (a) (b) schematic of the power combiners, (c) (d) phase response of the combiners, (e) (f) phase response of the filter loop, and (g) (h) band-pass filter response.

equivalent to the one obtained with an electrically long line, and therefore enlarges the electrical length of the filter loop as well (Fig. 7(e)). When the phase of the loop is zero, the feedback signal is constructively combined with the input, what happens at the two desired pass-bands, but at other intermediate frequencies as well (Fig. 7(g)). However, the slope in the phase curve of the proposed coupled lines (and any other broadband combiner) is flatter (Fig. 7(d)), and the electrical length of the loop is drastically reduced (Fig. 7(f)). Thus, spurious peaks do not appear in this case (Fig. 7(h)).

4. EXPERIMENTAL RESULTS

4.1. First-order Prototype

The theoretical principles presented above will be proved by means of a first-order active filter designed to operate at two frequencies: $f_1 = 800\,\text{MHz}$ and $f_2 = 1650\,\text{MHz}$. The circuit schematic is described in Fig. 8, and is based on the filter topology presented in Fig. 4(a).

It has been implemented using surface mounting devices over a microstrip substrate. The active stage has been designed by using the monolithic broadband high gain amplifier ERA-5+ from *Mini-Circuits*, which is already matched. The CRLH cell has been placed in the other branch as described in Fig. 2. Finally, a series resistive attenuator allows limiting the gain in the ring to avoid instabilities. The response of the coupled lines combiner is shown in Fig. 9. It has been intentionally designed to exhibit a higher coupling coefficient

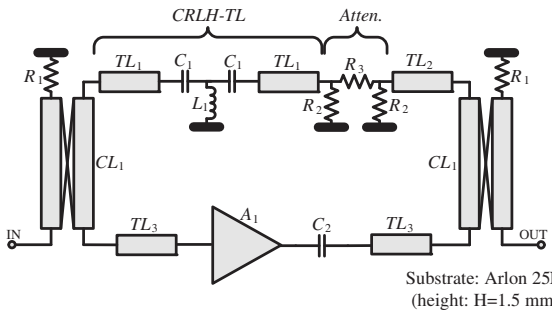

List of components

Name	Value
CL_1	w=3.1 mm, l=30 mm, s=0.2 mm
TL_1	w=3.4 mm, l=9.5 mm
TL_2	w=3.4 mm, l=13.6 mm
TL_3	w=3.4 mm, l=20.5 mm
L_1	8.2 nH (0402)
C_1	3.3 pF (0402)
C_2	100 pF (0402)
R_1	51 Ω (1206)
R_2	62 Ω (1206)
R_3	130 Ω (1206)
A_1	Mini-Circuits ERA-5+

Figure 8. Circuit schematic and list of components of the first-order dual-band active filter prototype. The transmission lines are characterized by the width w and the length l. The coupled lines also include the separation gap s. The biasing network has been omitted for simplicity.

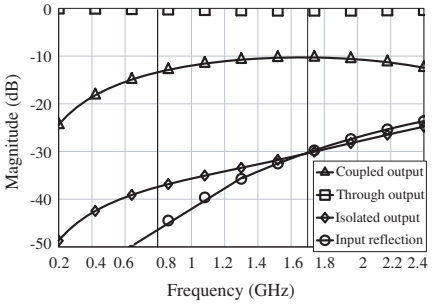

Figure 9. Simulated response of the coupled lines power combiners.

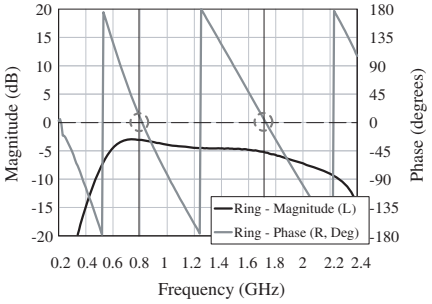

Figure 10. Simulated response (magnitude and phase) of the filter loop.

(i.e., α_i) at the higher frequency, in order to compensate the frequency-descendent slope of the amplifier gain and obtain a more symmetrical filter response.

The response of the ring is shown in Fig. 10. It can be seen how the phase has been adjusted to 0 deg. at the two desired frequencies. Furthermore, no other intermediate frequencies fulfill the condition of 0 deg, so no spurious peaks appear in the filter response. With respect to the magnitude, it has been limited to be under 0 dB in order to avoid stability problems, as it was explained in Section 3.2.

Finally, the measured filter response is shown in Figs. 11 and 12, and the numerical results are summarized in Table 1. There is a good agreement between the simulated and measured results. The filter response is very symmetrical, with gain values of 3.8 dB and 3.5 dB respectively. The relative bandwidths at each frequency band are 5.8% and 4.4% respectively. All the reflections coefficients are lower than -9 dB.

With respect to the noise performance, the filter noise figure mainly depends on the first coupling coefficient and on the amplifier gain (see (9) or (10)). As the input coupling lines present a low coupling coefficient (from Fig. 10, $\alpha_1(f_1) = -13.5$ dB and $\alpha_1(f_2) = -10.3$ dB), the only way to reduce the noise will be by making a proper choice of the amplifier noise figure. Three prototypes with three different monolithic amplifiers (ERA-5+, ERA-8+ and PMA-545+ from *Minicircuits*) have also been implemented. As it can be seen in Fig. 13, the noise figure of the filter depends on the amplifier choice, as it was expected.

Table 1. Measured parameters of the three filter prototypes.

Magnitude	1st order		2nd order		3rd order	
Frequency	800 MHz	1650 MHz	800 MHz	1750 MHz	800 MHz	1750 MHz
Gain	3.8 dB	3.5 dB	5.0 dB	2.8 dB	15.5 dB	11.5 dB
$\|s_{11}\|$	<-13 dB	<-10 dB	<-22 dB	<-11 dB	<-23 dB	<-8 dB
$\|s_{22}\|$	<-17 dB	<-9 dB	<-11 dB	<-11 dB	<-26 dB	<-10 dB
BW (3 dB)	47 MHz	72 MHz	70 MHz	160 MHz	83 MHz	202 MHz
BW (%)	5.8%	4.8%	8.8%	9.1%	10.4%	11.5%
Group delay	-1.4 ns	3.3 ns	8.7 ns	3.7 ns	10.3 ns	4.8 ns

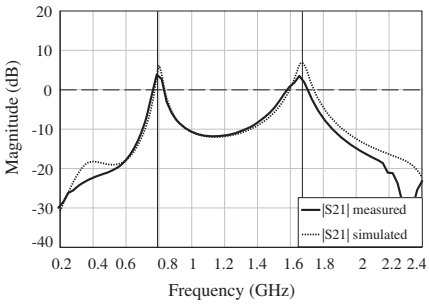

Figure 11. Transmission coefficient of the first-order active filter.

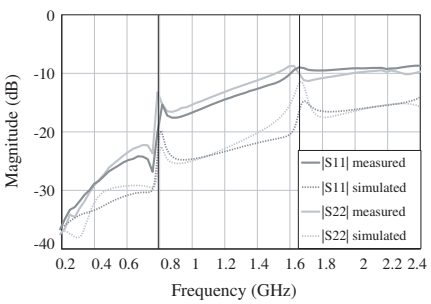

Figure 12. Reflection coefficients of the first-order active filter.

4.2. Multiple Order Prototypes

When stronger requirements in terms of selectivity, bandwidth or ripple are given, multiple order filters may be needed in order to satisfy all these conditions. In this case, higher order structures can be easily obtained just by cascading more than one ring resonators, as it was exposed in Fig. 5. This section shows the experimental results obtained with two prototypes, based on second and third-order topologies. The goal is to improve the rejection and increase the bandwidth of the first-order filter presented in the previous subsection, by adding extra ring resonators to this filter. The circuit schematic of the second-

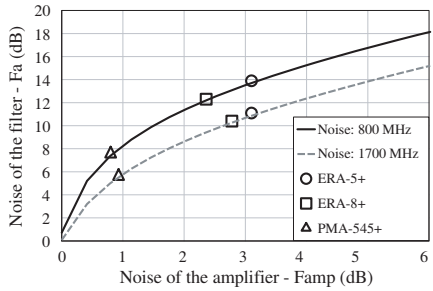

Figure 13. Simulated noise curves of the filter F_a as a function of the noise figure of the amplifier F_{amp} (from 9), and measured noise performance obtained with the ERA-5+, ERA-8+ and PMA-545+ amplifiers.

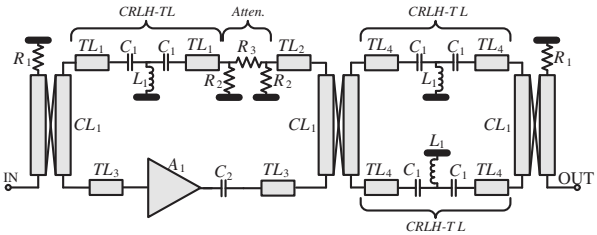

List of components

Name	Value
CL_1	w=3.1 mm, l=32 mm, s=0.2 mm
TL_1	w=3.4 mm, l=9.5 mm
TL_2	w=3.4 mm, l=13.6 mm
TL_3	w=3.4 mm, l=20.5 mm
TL_4	w=3.4 mm, l=12.1 mm
L_1	8.2 nH (0402)
C_1	3.3 pF (0402)
C_2	100 pF (0402)
R_1	51 Ω (1206)
R_2	62 Ω (1206)
R_3	270 Ω (1206)
A_1	Mini-Circuits ERA-5+

Figure 14. Circuit schematic and list of components of the second-order dual-band active filter prototype.

order prototype is shown in Fig. 14. A passive ring resonator based on two CRLH lines has been coupled to the output of the active filter characterized in the previous subsection. The measured results are plotted in Figs. 15 and 16 and summarized in Table 1.

Although the gain has not been significantly increased, the rejection at intermediate frequencies has been improved more than 15 dB compared with the first-order implementation. Furthermore, the bandwidth in this case is around 9% in both bands, which has been widely increased with respect to the previous case. Other characteristics, such as reflection coefficients and noise figure have not suffered significant variations.

On the other hand, the third-order schematic is shown in Fig. 17. An extra active stage has been added at the output of the second-order filter. As shown in Figs. 18 and 19, the gain at both pass-bands has been improved around 10 dB with respect to the second-

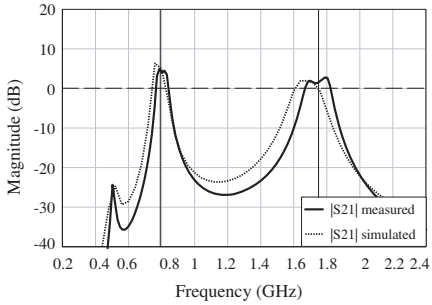

Figure 15. Transmission coefficient of the second-order active filter.

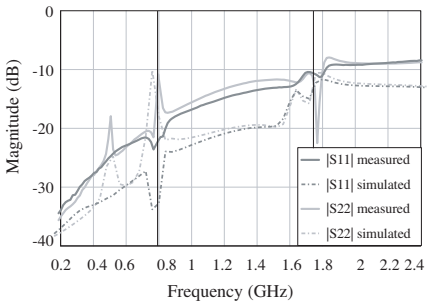

Figure 16. Reflection coefficients of the second-order active filter.

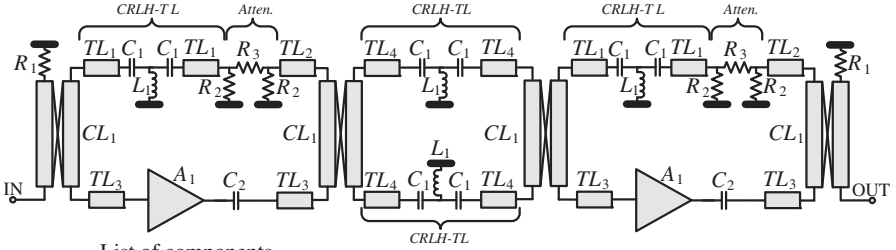

List of components

Name	Value	Name	Value
CL_1	w=3.1 mm, l=29 mm, s=0.2 mm	C_1	3.3 pF (0402)
TL_1	w=3.4 mm, l=9.5 mm	C_2	100 pF (0402)
TL_2	w=3.4 mm, l=13.6 mm	R_1	51 Ω (1206)
TL_3	w=3.4 mm, l=20 mm	R_2	91 Ω (1206)
TL_4	w=3.4 mm, l=12.1 mm	R_3	270 Ω (1206)
L_1	8.2 nH (0402)	A_1	Mini-Circuits ERA-5+

Substrate: Arlon 25N (height: H=1.5 mm, permittivity: ε_r=3.38)

Figure 17. Circuit schematic and list of components of the third-order dual-band active filter prototype.

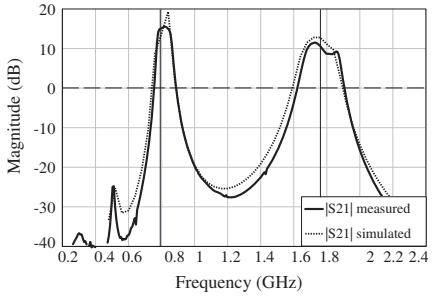

Figure 18. Transmission coefficient of the third-order active filter.

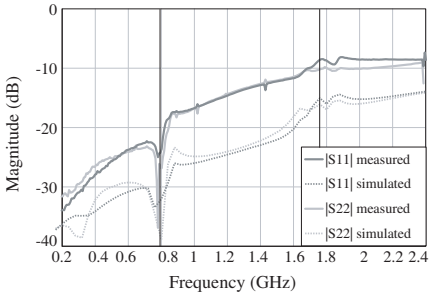

Figure 19. Reflection coefficients of the third-order active filter.

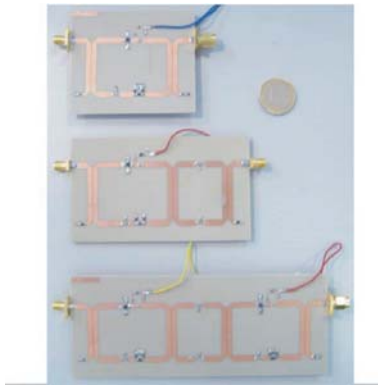

Figure 20. Photographs of the first-, second- and third-order dual-band active filter prototypes.

order filter, but with the cost of doubling the power consumption. The fractional bandwidth in this case is around 11% in both bands. The reflection coefficients and the noise figure are very similar to the previous implementations. All the numerical results are summarized in Table 1. Finally, the photograph of the three implemented dual-band active filters is shown in Fig. 20.

5. CONCLUSION

The design of multiple order and dual-band active filters by means of CRLH transmission lines in an active ring resonator topology has been treated in this paper. The non-linear phase response exhibited by the CRLH lines is used to adjust the electrical length of the ring at two arbitrary frequencies. In addition to its basic operation principles, other important issues, such as stability and noise, have been analyzed.

The combination of signals by means of coupled lines allows the implementation of very compact devices. On the other hand, high order structures can be easily designed just by coupling different ring sections. Furthermore, no spurious peaks at intermediate frequencies appear in the frequency response as they appear with other dual-band topologies based on dual-band combiners.

Finally, all the theoretical principles agree with the conclusions taken from the measurements of three different prototypes. These filters operate at the same frequencies, and are based on first-, second- and third-order topologies respectively. It has been shown how the selectivity and the bandwidth can be controlled by adding additional stages.

ACKNOWLEDGMENT

This work has been granted by the Spanish Ministerio de Educación y Ciencia (MEC) under Projects TEC2006-13248-C04-04/TCM, Consolider CSD2008-0068 and TEC2009-14525-C02-01, and by the Instituto Geográfico Nacional (IGN) under grant FOM/3740/2007.

REFERENCES

1. Lai, A., T. Itoh, and C. Caloz, "Composite right/left-handed transmission line metamaterials," *IEEE Microwave Magazine*, Vol. 5, No. 3, 34–50, September 2004.
2. Jie, X., C. Luo, and X. Zhao, "A dual-frequency microstrip antenna based on an unbalanced composite right/left-handed transmission line," *Microw. Opt. Technol. Lett.*, Vol. 50, No. 3, 767–771, January 2008.
3. Herraiz-Martinez, F. J., V. Gonzalez-Posadas, L. E. Garcia-Muñoz, and D. Segovia-Vargas, "Multifrequency and dual-mode patch antennas partially filled with left-handed structures," *IEEE Trans. Antennas Propag.*, Vol. 56, No. 8, 2527–2539, August 2008.
4. Yu, A., F. Yang, and A. Elsherbeni, "A dual-band circularly polarized ring antenna based on composite right and left handed metamaterials," *Progress In Electromagnetics Research*, PIER 78, 73–81, 2008.
5. Hsiang, L. I., M. De Vicentis, C. Caloz, and T. Itoh, "Arbitrary dual-band components using composite right/left-handed transmission lines," *IEEE Trans. Microw. Theory Tech.*, Vol. 52, No. 8, 1142–1149, April 2004.
6. Lin, X. Q., R. P. Liu, X. M. Yang, J. X. Chen, X. X. Yin, Q. Cheng, and T. J. Cui, "Arbitrarily dual-band components using simplified structures of conventional CRLH TLs," *IEEE Trans. Microw. Theory Tech.*, Vol. 54, No. 7, 2902–2909, July 2006.
7. Castro-Galan, D., L. E. Garcia-Muñoz, D. Segovia-Vargas, and V. Gonzalez-Posadas, "Diversity monopulse antenna based on a dual-frequency and dual-mode CRLH rat-race coupler," *Progress In Electromagnetics Research B*, Vol. 14, 87–106, 2009.
8. Hayati, M. and M. Nosrati, "Loaded coupled transmission line approach of left-handed (LH) structures and realization of a highly compact dual-band branch-line coupler," *Progress In Electromagnetics Research C*, Vol. 10, 75–86, 2009.
9. Dupuy, A. A., K. M. Leong, and T. Itoh, "Class-F power amplifier using a multi-frequency composite right/left-handed transmission

line harmonic tuner," *IEEE MTT-S Int. Microw. Symp. Dig.*, June 2005.

10. Jimenez-Martin, J. L., V. Gonzalez-Posadas, J. E. Gonzalez-Garcia, F. J. Arques-Orobon, L. E. Garcia-Muñoz, and D. Segovia-Vargas, "Dual band high efficiency class CE power amplifier based on CRLH diplexer," *Progress In Electromagnetics Research*, PIER 97, 217–240, 2009.
11. Mata-Contreras, J., T. M. Martin-Guerrero, and C. Camacho-Peñalosa, "Distributed amplifiers with composite left/right-handed transmission lines," *Microw. Opt. Technol. Lett.*, Vol. 48, No. 3, 609–613, January 2006.
12. Garcia-Perez, O., A. Garcia-Lamperez, V. Gonzalez-Posadas, M. Salazar-Palma, and D. Segovia-Vargas, "Dual-band recursive active filters with composite right/left-handed transmission lines," *IEEE Trans. Microw. Theory Tech.*, Vol. 57, No. 5, 1180–1187, May 2009.
13. Chang, C.-Y. and T. Itoh, "Microwave active filters based on coupled negative resistance method," *IEEE Trans. Microw. Theory Tech.*, Vol. 38, No. 12, 1879–1884, December 1990.
14. Lucyszyn, S. and I. D. Robertson, "Monolithic narrow-band filter using ultrahigh-Q tunable active inductors," *IEEE Trans. Microw. Theory Tech.*, Vol. 42, No. 12, 2617–2622, December 1994.
15. Rauscher, C., "Microwave active filters based on transversal and recursive principles," *IEEE Trans. Microw. Theory Tech.*, Vol. 33, No. 12, 1350–1360, December 1985.
16. Matsuo, M., H. Yabuki, and M. Makimoto, "Dual-mode stepped-impedance ring resonator for bandpass filter applications," *IEEE Trans. Microw. Theory Tech.*, Vol. 49, No. 7, 1235–1240, July 2001.
17. Hsie, L.-H. and K. Chang, "Dual-mode quasi-elliptic-function band-pass filters using resonators with enhanced-coupling tuning stubs," *IEEE Trans. Microw. Theory Tech.*, Vol. 50, No. 5, 1340–1345, May 2002.
18. Mohd-Salleh, M. K., G. Prigent, O. Pigaglio, and R. Crampagne, "Quarter-wavelength side-coupled ring resonator for bandpass filters," *IEEE Trans. Microw. Theory Tech.*, Vol. 56, No. 1, 156–162, January 2008.
19. Huang, T.-H., H.-J. Chen, C.-S. Chang, L.-S. Chen, Y.-H. Wang, and M.-P. Houng, "A novel compact ring dual-mode filter with adjustable second-passband for dual-band applications," *IEEE Microw. Wireless Comp. Lett.*, Vol. 16, No. 6, 360–362, June 2006.

20. Garcia-Lamperez, A. and M. Salazar-Palma, "Dual band filter with split-ring resonators," *IEEE MTT-S Int. Microw. Symp. Dig.*, 519–522, June 2006.
21. Chen, Z.-X., X.-W. Dai, and C.-H. Liang, "Novel dual-mode dual-band bandpass filter using double square-loop structure," *Progress In Electromagnetics Research*, PIER 77, 409–416, 2007.
22. Fan, J.-W., C.-H. Liang, and X.-W. Dal, "Design of cross-coupled dual-band filter with equal length split-ring resonators," *Progress In Electromagnetics Research*, PIER 75, 285–293, 2007.
23. Xue, W., C.-H. Liang, X.-W. Dai, and J.-W. Fan, "Design of miniature planar dual-band filter with 0 feed structures," *Progress In Electromagnetics Research*, PIER 77, 493–499, 2007.
24. Wu, G.-L., W. Mu, X.-W. Dai, and Y.-C. Jiao, "Design of novel dual-band bandpass filter with microstrip meander-loop resonator and CSRR DGS," *Progress In Electromagnetics Research*, PIER 78, 17–24, 2008.
25. Luo, S. and L. Zhu, "A novel dual-mode dual-band bandpass filter based on a single ring resonator," *IEEE Microw. Wireless Comp. Lett.*, Vol. 19, No. 8, 497–499, August 2009.
26. Nenert, L., D. Denis, L. Billonnet, B. Jarry, and P. Guillon, "Actively compensated planar ring resonator structures suitable for bandstop and bandpass filters," *IEEE Russia Conf. High. Power Microw. Electron.: Measur., Identific. and Applic.*, MIA-ME'99, 1137–1142, September 1999.
27. Billonnet, L., B. Jarry, and P. Guillon, "Stability diagnosis of microwave recursive structures using the NDF methodology," *IEEE MTT-S Int. Microw. Symp. Dig.*, Vol. 3, 1419–1422, May 1995.
28. Ezzedine, H., L. Billonnet, B. Jarry, and P. Guillon, "Optimization of noise performance for various topologies of planar microwave active filters using noise wave techniques," *IEEE Trans. Microw. Theory Tech.*, Vol. 46, No. 12, 2484–2492, December 1998.